

14-3-3 adaptor proteins recruit AID to 5'-AGCT-3'-rich switch regions for class switch recombination

Zhenming Xu¹, Zsolt Fulop¹, Guikai Wu², Egest J. Pone¹, Jinsong Zhang¹, Thach Mai¹, Lisa M. Thomas¹, Ahmed Al-Qahtani¹, Clayton A. White¹, Seok-Rae Park¹, Petra Steinacker³, Zenggang Li⁴, John Yates, III⁵, Bruce Herron⁶, Markus Otto³, Hong Zan¹, Haian Fu⁴ & Paolo Casali¹

¹Institute for immunology, School of Medicine and School of Biological Sciences, University of California, Irvine, CA 92697-4120. ²Department of Biological Chemistry, School of Medicine, University of California, Irvine, CA 92697. ³Department of Neurology, University of Ulm, 89075 Ulm, Germany. ⁴Department of Pharmacology, School of Medicine, Emory University, Atlanta, GA 30322. ⁵Department of Chemical Physiology, The Scripps Research Institute, La Jolla, CA 92037. ⁶Wadsworth Center, New York State Department of Health, Albany, NY 12201. Correspondence should be addressed to Paolo Casali (email: pcasali@uci.edu; phone: 949-824-9648; fax: 949-824-2305).

LIST OF SUPPLEMENTARY MATERIALS

Supplementary Figure 1. 5'-AGCT-3' is an evolutionarily conserved motif recurring at a high frequency in S regions of the IgH locus.

Supplementary Figure 2. 14-3-3 bind to and are eluted from an affinity column bearing the [5'-AGCT-3']₃-24 bp oligonucleotide.

Supplementary Figure 3. 14-3-3 isoforms and their blocking by difopein.

Supplementary Figure 4. Blocking 14-3-3 by difopein inhibits CSR in human and mouse B cells.

Supplementary Figure 5. Normal B and T lymphocyte development, T cell viability and germinal center development in 14-3-3 $\gamma^{-/-}$ mice.

Supplementary Figure 6. Normal B and T lymphocyte development, T cell viability and germinal center development in 14-3-3 $\sigma^{+/Er}$ mice.

Supplementary Figure 7. Direct interaction of 14-3-3 ζ with AID in the nucleus.

Supplementary Figure 8. Direct interaction of 14-3-3 adaptors with AID and PKA-C α and specific interaction of difopein with 14-3-3.

Supplementary Figure 9. 14-3-3 enhance AID-mediated dC DNA deamination in a dose-dependent fashion.

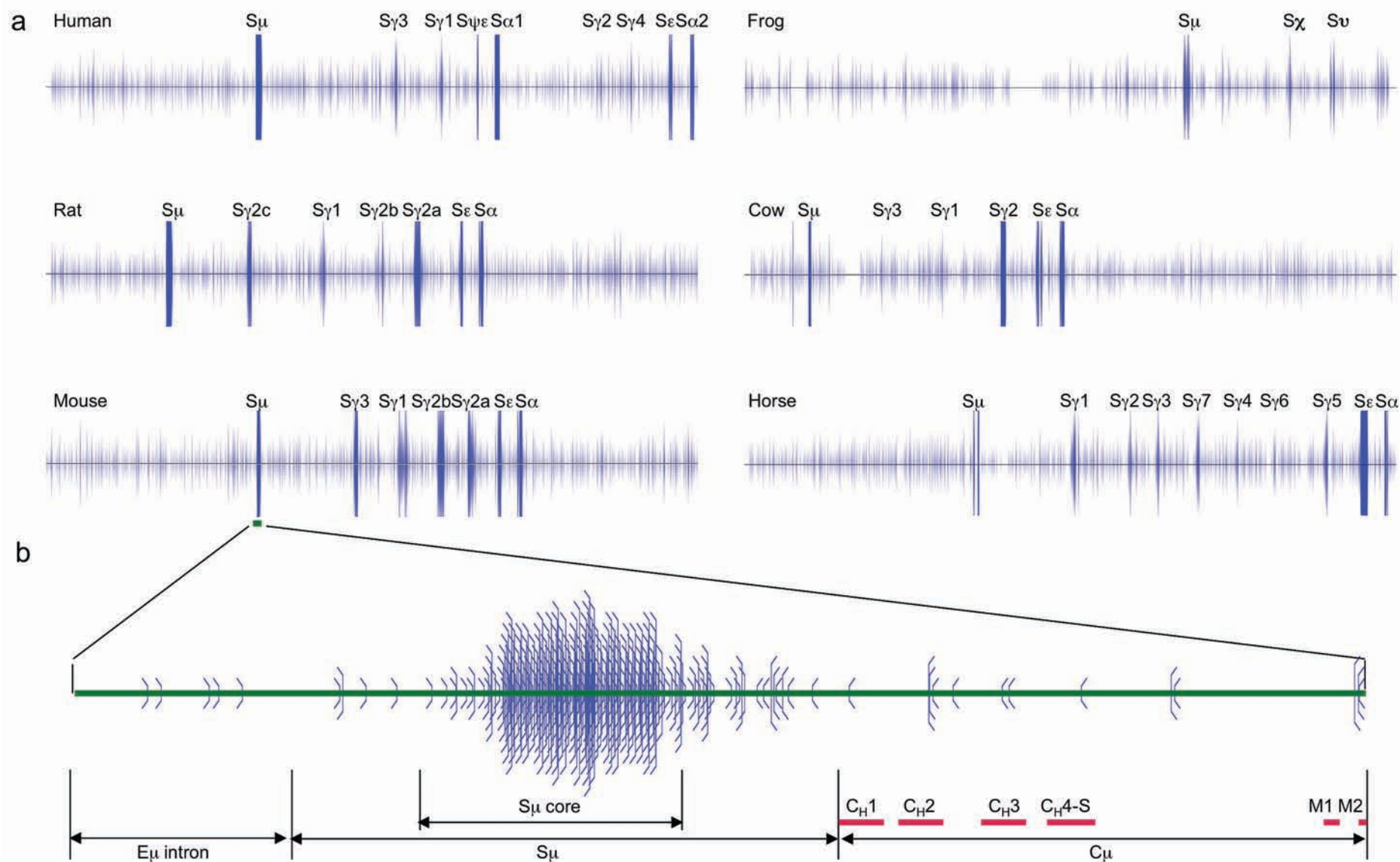
Supplementary Table 1. Frequency of the 5'-AGCT-3' occurrence in IgH S region DNA.

Supplementary Table 2. Binding of 14-3-3 proteins in human B cells to [5'-AGCT-3']₃-24 bp oligonucleotide.

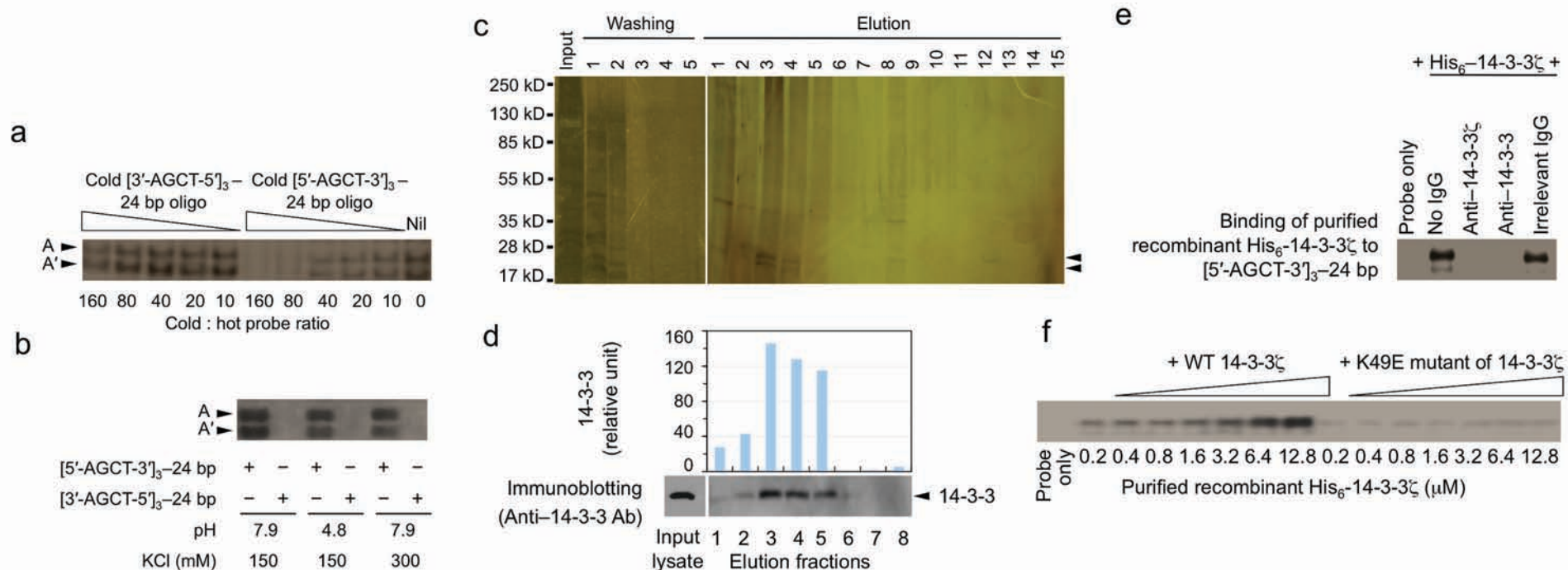
Supplementary Table 3. Oligonucleotide sequences.

Supplementary Table 4. Antibodies.

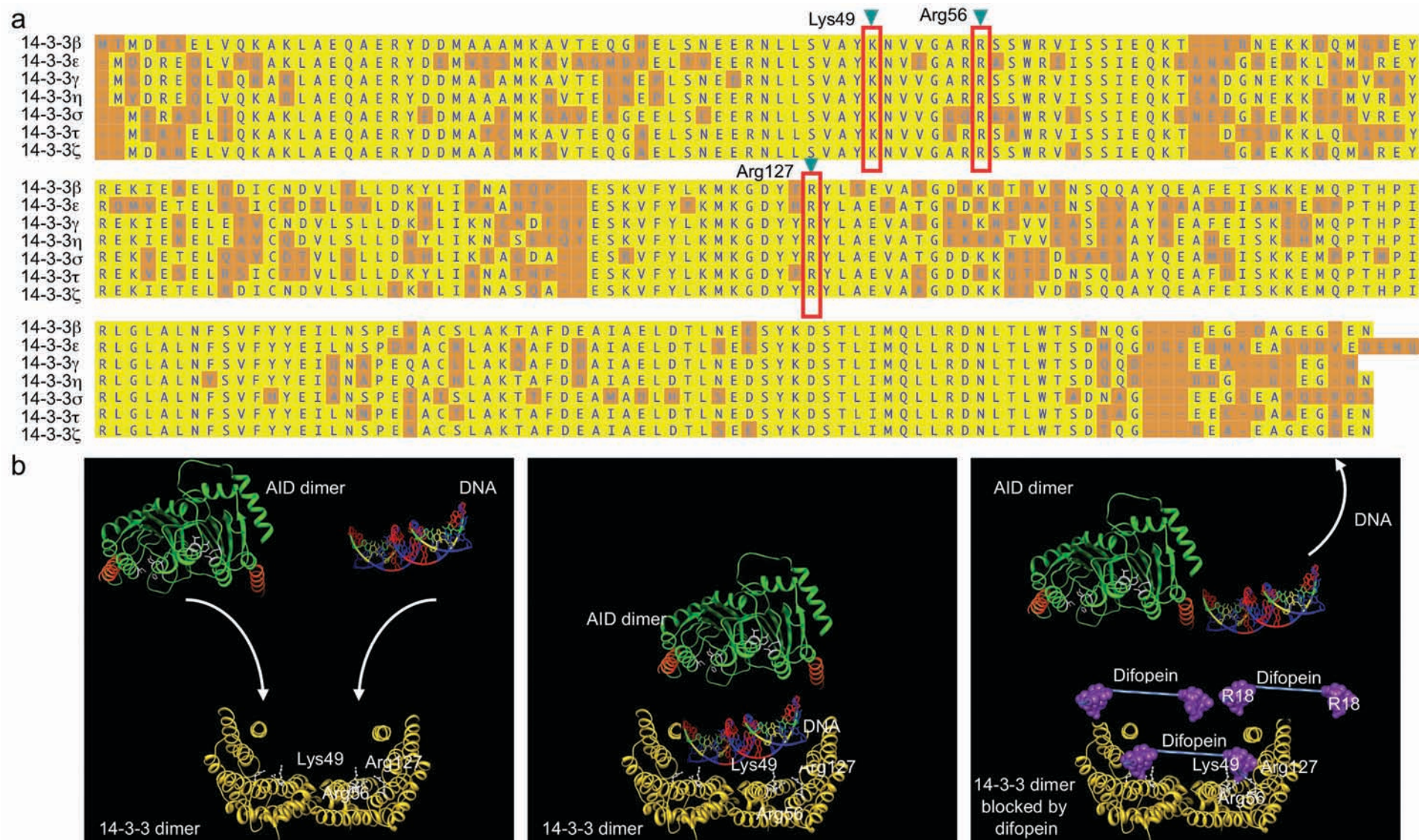
Supplementary Methods.



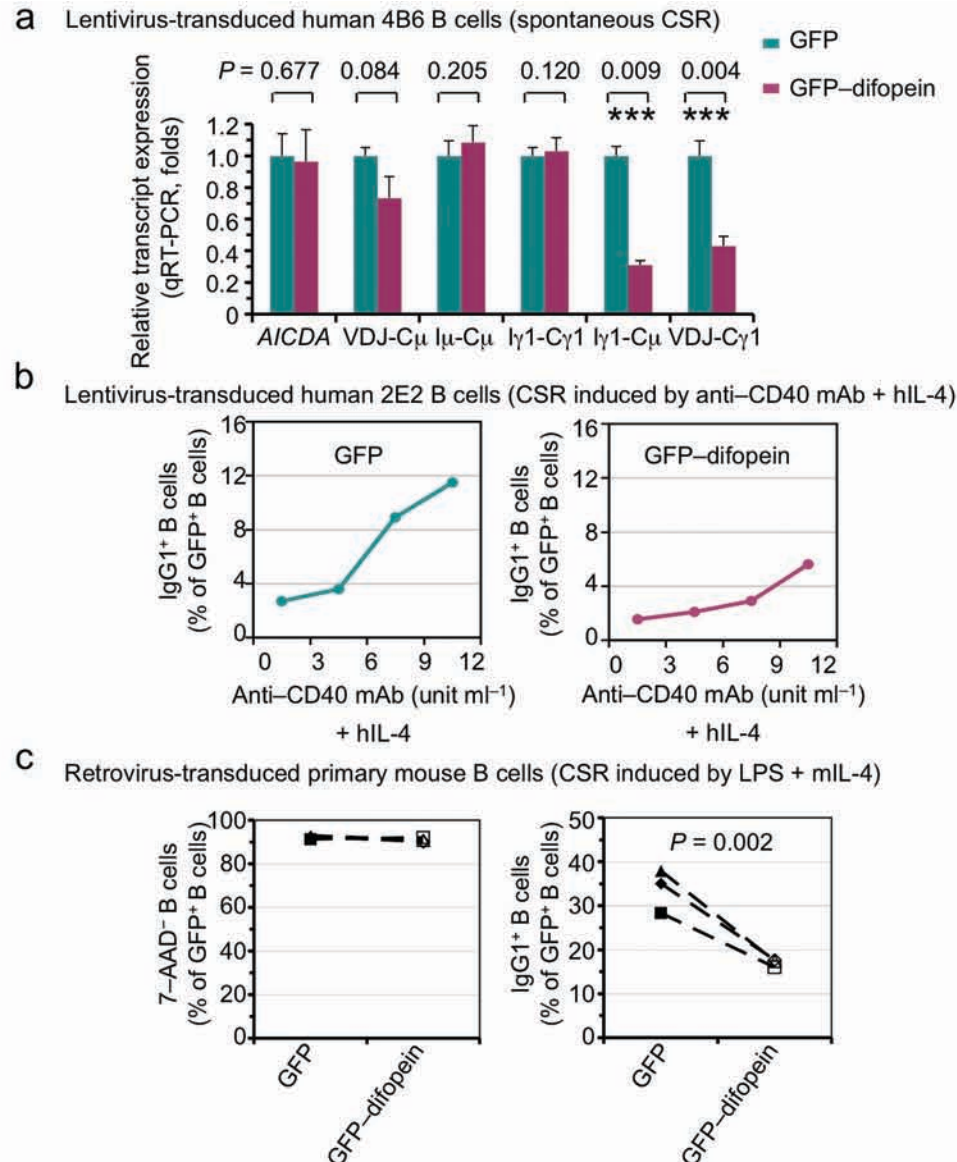
Supplementary Figure 1. 5'-AGCT-3' is an evolutionarily conserved motif recurring at a high frequency in S regions of the IgH locus. (a) High density of 5'-AGCT-3' motifs in S regions of the IgH locus in species that support CSR, from *Xenopus tropicalis* to human. Each 5'-AGCT-3' motif in both strands of 400 kb DNA that includes all D $_H$ and J $_H$ gene segments, S and C $_H$ regions is depicted as a vertical line. Lines are stacked when multiple 5'-AGCT-3' motifs are closely spaced. The graphs were generated using MacVector® software (MacVector, Inc.). (b) Magnified map of the mouse *Igh* DNA from the end of the J $_H$ 4 gene segment to C μ region, including the E μ intron, S μ and the C μ 1, C μ 2, C μ 3, C μ 4-S, M1 and M2 exons of C μ , shows the high density of 5'-AGCT-3' motifs in the S μ core.



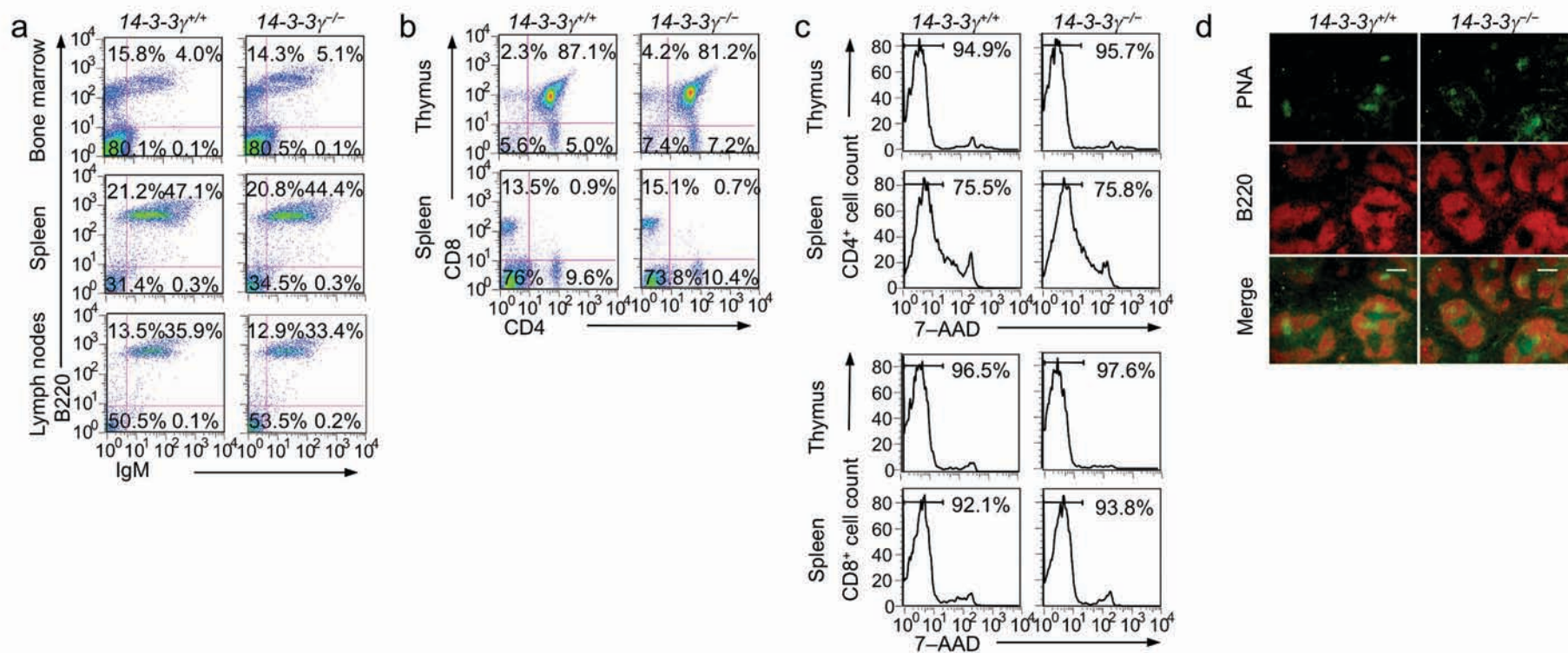
Supplementary Figure 2. 14-3-3 proteins bind to [5'-AGCT-3']₃-24 bp oligonucleotide. (a) Binding of 4B6 B cell nuclear extract proteins to ³²P-end labeled (hot) [5'-AGCT-3']₃-24 bp oligonucleotide was competed by non-radiolabeled (cold) [5'-AGCT-3']₃-24 bp oligonucleotide, but not cold [3'-AGCT-5']₃-24 bp oligonucleotide. (b) EMSA involving 4B6 B cell nuclear extracts and [5'-AGCT-3']₃-24 bp or [3'-AGCT-5']₃-24 bp under different pH and ionic strength. (c) 14-3-3 bind to and are eluted from an affinity column bearing the [5'-AGCT-3']₃-24 bp oligonucleotide. SDS-PAGE and silver staining analysis of nuclear proteins prepared from spontaneously switching human IgM⁺ IgD⁺ 4B6 B cells and enriched by NeutrAvidin agarose beads bearing the biotinylated [5'-AGCT-3']₃-24 bp oligonucleotide. 4B6 B cell nuclear extract protein solution (40 ml) was applied to 1 ml of NeutrAvidin beads bearing the [5'-AGCT-3']₃-24 bp oligonucleotide in the presence of a 100-fold molar excess of the control [3'-AGCT-5']₃-24 bp oligonucleotide. After extensive washing (100 ml of the pass-through was collected in five 20-ml fractions), bound proteins were eluted by 15 ml of high salt (600 mM) elution buffer and collected in 1-ml fractions. Full-length SDS-PAGE (Protean® II, xi, Bio-Rad Laboratories) and silver staining were performed to analyze proteins in the input lysate, five washing fractions and fifteen elution fractions. The three main elution fractions (#3, #4 and #5) showed prominent protein bands at 28 kD (arrowheads). (d) Identification of 14-3-3 proteins in the input 4B6 B cell nuclear lysate and in the first eight fractions eluted from the [5'-AGCT-3']₃-24 bp oligonucleotide affinity column by SDS-PAGE (Mini Protean®, Bio-Rad Laboratories) and immunoblotting using an Ab recognizing all 14-3-3 isoforms (bottom panel); the seven 14-3-3 isoforms segregate within one band in mini-protein gels due to their narrow size range, 27.8 – 29.2 kD). Signals were quantified using ImageJ software (NIH) and are depicted as relative levels of 14-3-3 proteins (bars, top panel). (e) EMSA analysis of binding of purified recombinant His₆-14-3-3ζ to the [5'-AGCT-3']₃-24 bp oligonucleotide probe and blocking of the binding by an Ab to 14-3-3ζ or an Ab to all 14-3-3 isoforms or control IgG with irrelevant specificities. (f) EMSA analysis of the binding of two-fold increasing amounts of purified recombinant His₆-14-3-3ζ or its K49E mutant to the [5'-AGCT-3']₃-24 bp oligonucleotide probe.



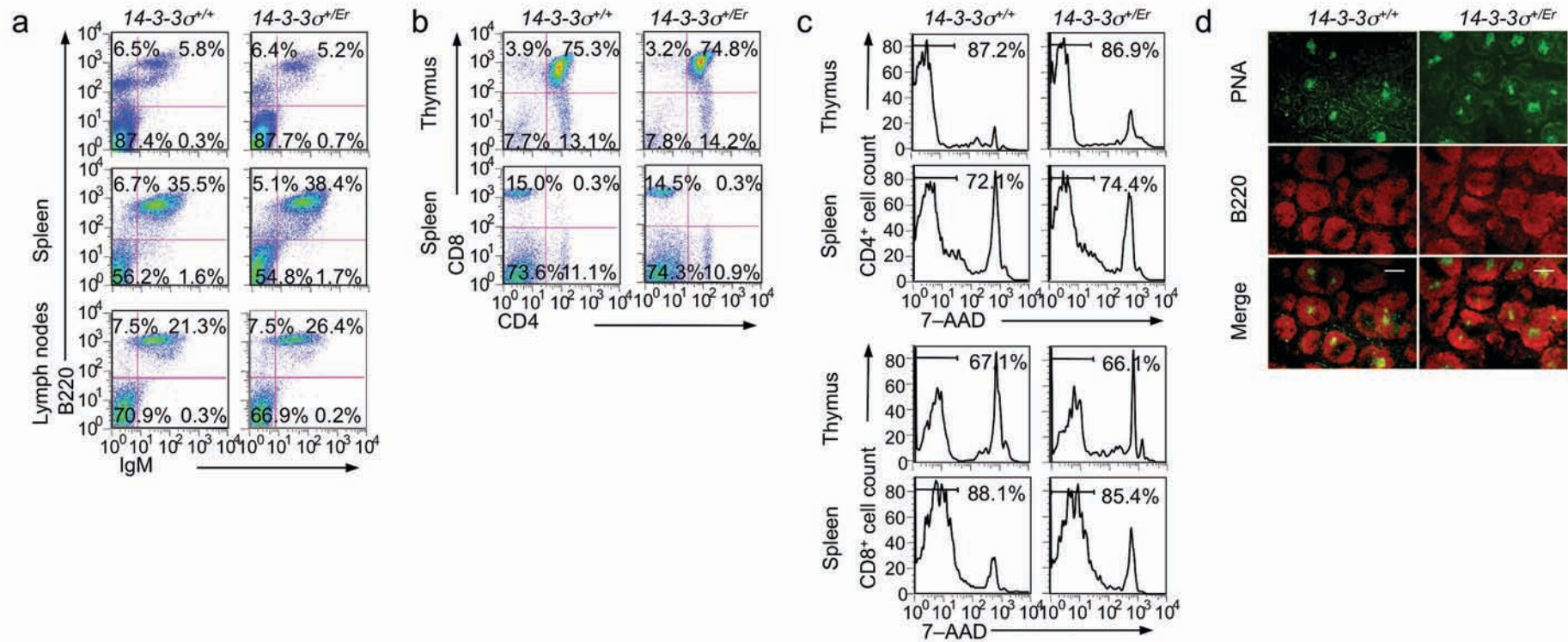
Supplementary Figure 3. 14-3-3 isoforms and their blocking by difopein. **(a)** High homology of the seven human 14-3-3 isoforms. The protein alignment was generated using Lasergene® software (DNASTAR, Inc) and is a slight modification of a crystal structure-based sequence alignment of 14-3-3 isoforms (*Semin. Cancer. Biol.* 16: 173–182, 2006). The three highly conserved and positively charged amino acids Lys49, Arg56 and Arg127 in the amphipathic groove likely mediate binding of 14-3-3 to 5'-AGCT-3' DNA. **(b)** Schematic depiction of blocking of 14-3-3 by difopein. All 14-3-3 isoforms form cup-shaped homo- and heterodimers (left panel, 14-3-3ζ in this case). A 14-3-3 dimer binds to 5'-AGCT-3'-rich DNA through the two amphipathic grooves and, by recruiting AID, brings DNA into proximity to the AID catalytic site (middle panel). Difopein contains two R18 monomers (purple), which bind to the 14-3-3 amphipathic grooves with high affinity and, therefore, block the binding of 14-3-3 to 5'-AGCT-3' DNA and decreasing the access of AID to 5'-AGCT-3' DNA (right panel). Graphs were rendered by UCSF Chimera (PDB ID: 14-3-3ζ alone or in association with difopein, 1A38; 5'-AGCT-3' DNA, 1EGW; AID, modeled using human APOBEC2, 2NYT; AID NES, modeled using human p53 NES, 1C26).



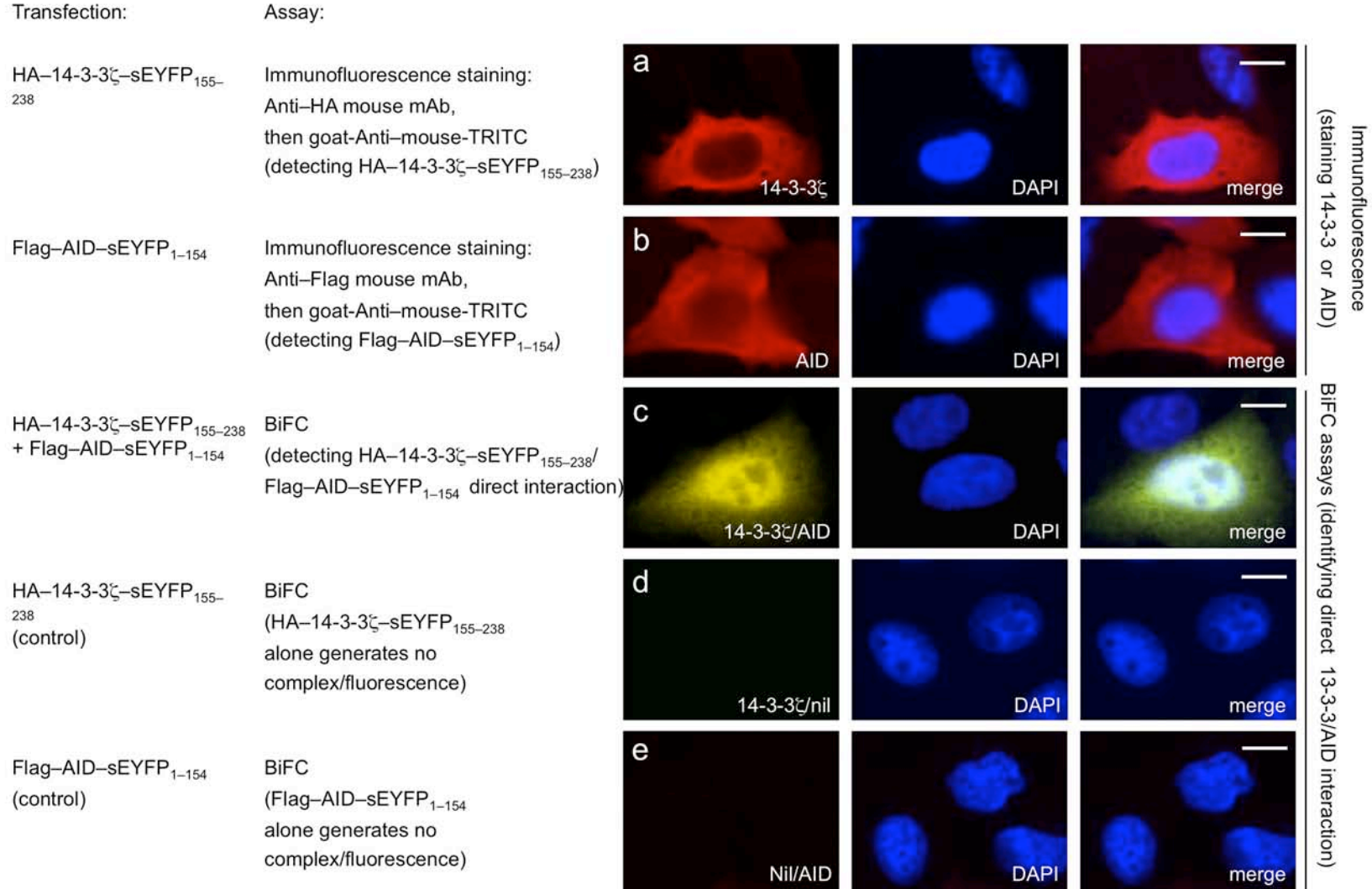
Supplementary Figure 4. Blocking 14-3-3 by difopein inhibits CSR in human and mouse B cells. **(a)** Human 4B6 B cells transduced with pFUW-GFP or pFUW-GFP-difopein lentivirus were analyzed for levels of *AICDA*, mature *V_HDJ_H-C μ* , germline *I μ -C μ* and *I γ 1-C γ 1*, circle *I γ 1-C μ* and mature post-recombination *V_HDJ_H-C γ 1* transcripts by real-time qRT-PCR (data are normalized to the level of *GAPDH* transcripts and depicted as ratio of levels in GFP-difopein-expressing 4B6 B cells to those in GFP-expressing 4B6 B cells, mean and s.d. of triplicate samples). Data depicting levels of *AICDA*, *V_HDJ_H-C μ* and germline *I μ -C μ* transcripts are the same as those presented in **Figure 5a**, panel [iii]. ***, $p < 0.01$. **(b)** Human 2E2 B cells transduced with pFUW-GFP or pFUW-GFP-difopein lentivirus were stimulated by different doses of mAb to hCD40 plus hIL-4 for 96 h and analyzed for surface IgG1 expression by flow cytometry. **(c)** Purified primary mouse B cells were activated by LPS for 24 h, transduced with pTAC-GFP or pTAC-GFP-difopein retrovirus and then stimulated by LPS plus mIL-4 for 72 h. B cells expressing GFP or GFP-difopein were analyzed by flow cytometry for viability (7AAD⁻, left panel) and surface IgG1 expression (right panel). Depicted are data of three independent experiments.



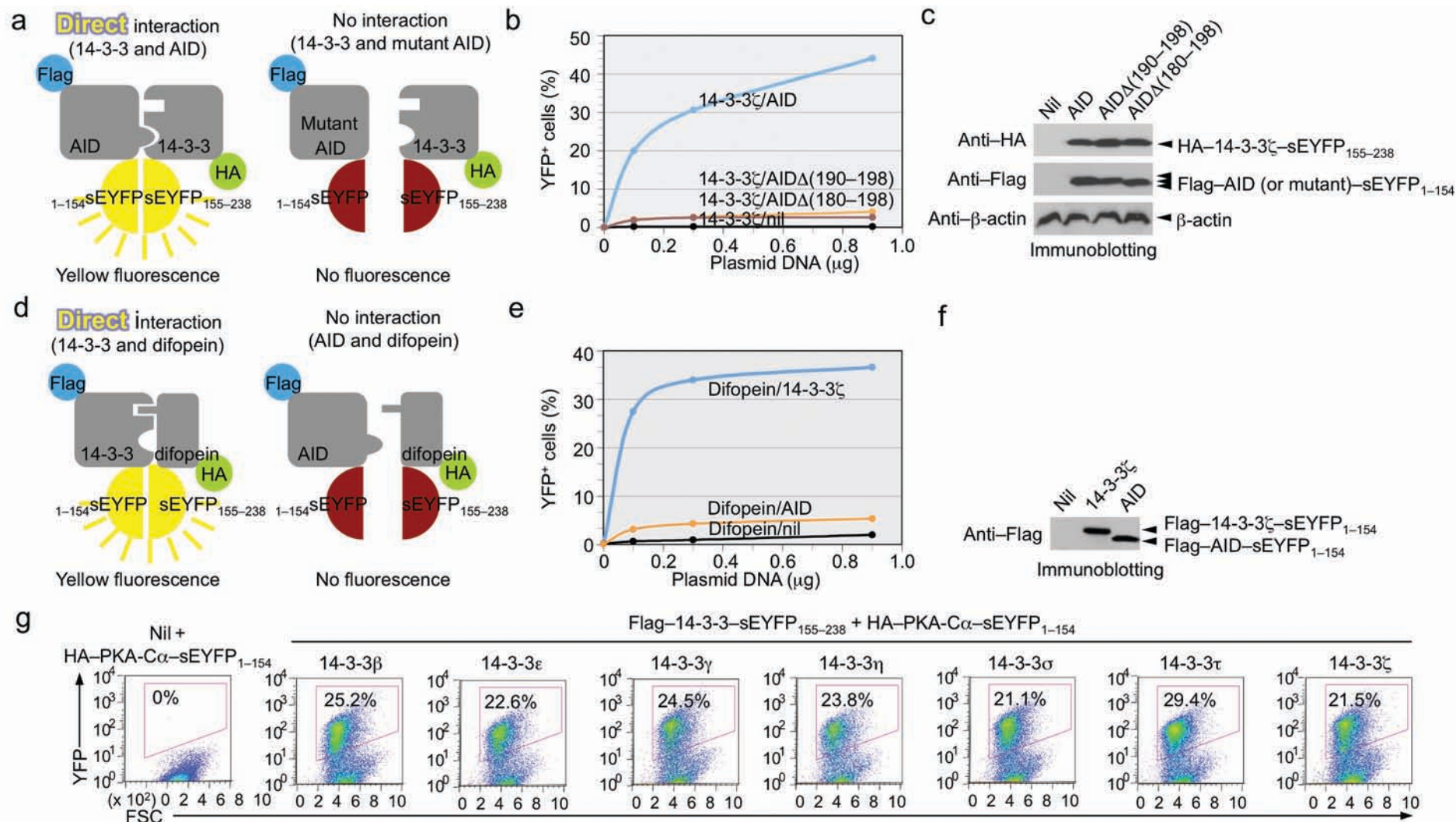
Supplementary Figure 5. Normal B and T lymphocyte development, T cell viability and germinal center development in 14-3-3 $\gamma^{-/-}$ mice. (a,b) Flow cytometry analysis of surface B220 and IgM expression in cells from bone marrow, spleen and lymph nodes (a), and surface CD4 and CD8 expression in cells from thymus and spleen (b) of 14-3-3 $\gamma^{-/-}$ and 14-3-3 $\gamma^{+/+}$ mouse littermates. (c) Flow cytometry analysis of viability (7-AAD⁻) of CD4⁺ and CD8⁺ T cells from thymus and spleen of 14-3-3 $\gamma^{-/-}$ and 14-3-3 $\gamma^{+/+}$ mouse littermates. (d) Spleen sections prepared from 14-3-3 $\gamma^{-/-}$ and 14-3-3 $\gamma^{+/+}$ mouse littermates 10 d after immunization with NP₁₆-CGG were stained with FITC-conjugated PNA (FITC-PNA, green) and PE-conjugated anti-B220 mAb (PE-anti-B220 mAb, red) to reveal germinal centers. Scale bar: 100 μ m.



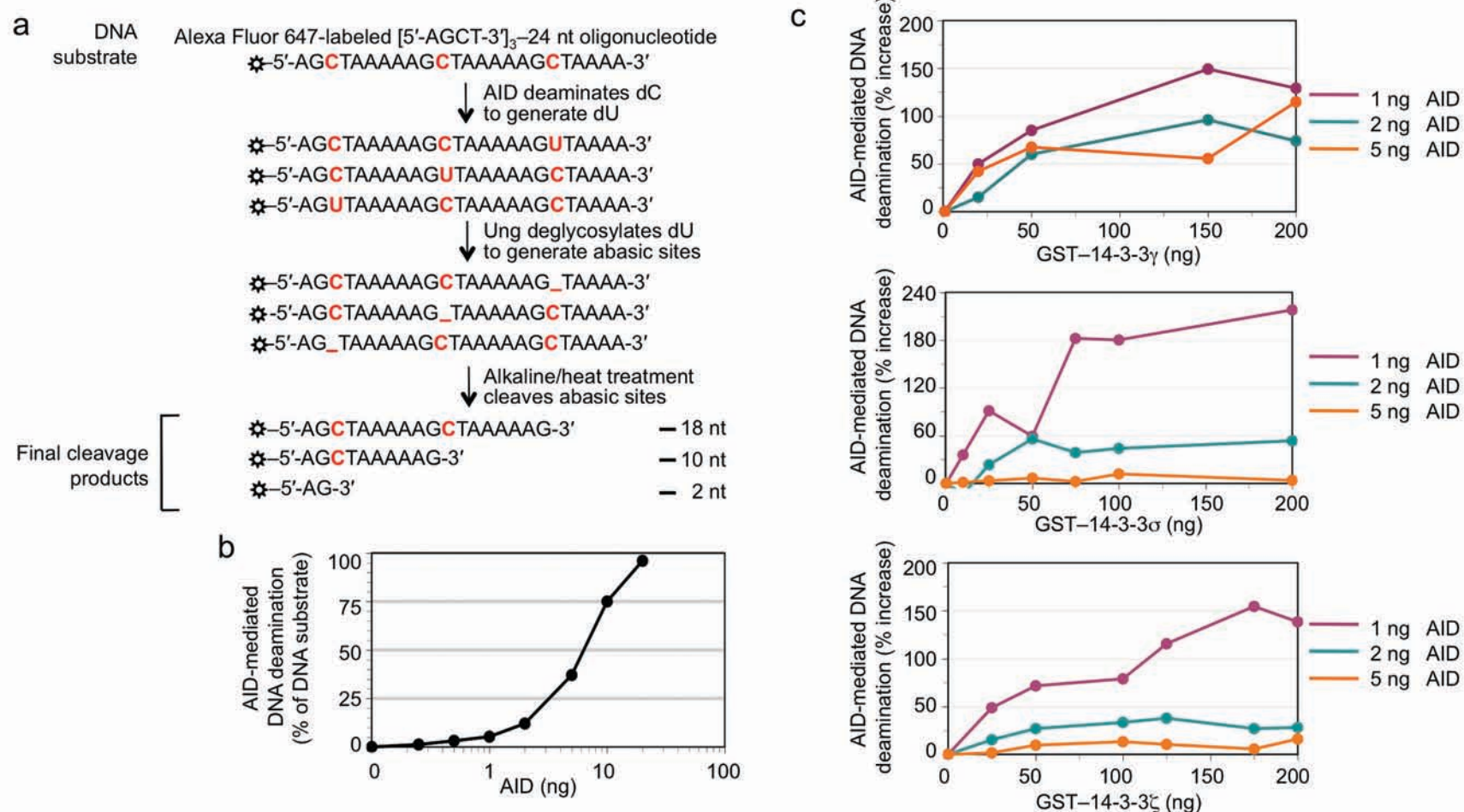
Supplementary Figure 6. Normal B and T lymphocyte development, T cell viability and germinal center development in 14-3-3 $\sigma^{+/Er}$ mice. (a,b) Flow cytometry analysis of surface B220 and IgM expression in cells from bone marrow, spleen and lymph nodes (a), and surface CD4 and CD8 expression in cells from thymus and spleen (b) of 14-3-3 $\sigma^{+/Er}$ and 14-3-3 $\sigma^{+/+}$ mouse littermates. (c) Flow cytometry analysis of viability (7-AAD⁻) of CD4-single positive and CD8-single positive T cells from thymus and spleen of 14-3-3 $\sigma^{+/Er}$ and 14-3-3 $\sigma^{+/+}$ mouse littermates. (d) Spleen sections prepared from 14-3-3 $\sigma^{+/Er}$ and 14-3-3 $\sigma^{+/+}$ mouse littermates 10 d after immunization with NP₁₆-CGG were stained with FITC-PNA (green) and PE-anti-B220 mAb (red) to reveal germinal centers. Scale bar: 100 μ m



Supplementary Figure 7. Direct interaction of 14-3-3 ζ with AID. (a,b) Immunofluorescence staining assays of the subcellular distribution of HA-14-3-3 ζ -sEYFP₁₅₅₋₂₃₈ (a) and Flag-AID-sEYFP₁₋₁₅₄ (b) expressed alone in HeLa cells 36 h after transfection. (c) BiFC assays of the direct interaction/complex formation of HA-14-3-3 ζ -sEYFP₁₅₅₋₂₃₈ and Flag-AID-sEYFP₁₋₁₅₄ co-expressed in HeLa cells 36 h after transfection, as revealed by fluorescence microscopy. SuperEYFP (sEYFP) is an EYFP variant that gives off three times of fluorescence per molecule than commonly used EYFP. (d,e) Expression of HA-14-3-3 ζ -sEYFP₁₅₅₋₂₃₈ (d) or Flag-AID-sEYFP₁₋₁₅₄ (e) alone did not give rise to any 14-3-3/AID complex, thereby giving off no yellow fluorescence. Scale bars, 5 μ m.



Supplementary Figure 8. Direct interaction of 14-3-3 adaptors with AID and PKA-Cα and specific interaction of difopein with 14-3-3. **(a)** Schematics of BiFC assays to analyze direct interaction between 14-3-3 and wildtype AID or AID C-terminal truncation mutants. **(b)** BiFC assays of direct interaction of 14-3-3ζ with AID, but not AIDΔ(190-198) or AIDΔ(180-198). HeLa cells were transfected for 24 h with two plasmids that expressed HA-14-3-3ζ-sEYFP₁₅₅₋₂₃₈ and Flag-AID-sEYFP₁₋₁₅₄, Flag-AIDΔ(190-198)-sEYFP₁₋₁₅₄ or Flag-AIDΔ(180-198)-sEYFP₁₋₁₅₄, respectively (0.1, 0.3 or 0.9 μg of each plasmid, x-axis; pcDNA plasmid was added to make up for 2 μg of total DNA). Depicted is the proportion of HeLa cells that were YFP⁺ (one representative of three experiments). **(c)** Immunoblotting analysis of HeLa cells co-expressing HA-14-3-3ζ-sEYFP₁₅₅₋₂₃₈ (anti-HA) and Flag-AID-sEYFP₁₋₁₅₄ or Flag-AIDΔ(190-198)-sEYFP₁₋₁₅₄ or Flag-AIDΔ(180-198)-sEYFP₁₋₁₅₄ (anti-Flag) 24 h after transfection. **(d)** Schematics of BiFC assays to analyze direct interaction of difopein with 14-3-3 or AID. **(e)** BiFC assays of direct interaction of HA-difopein-sEYFP₁₅₅₋₂₃₈ with Flag-14-3-3ζ-sEYFP₁₋₁₅₄, but not Flag-AID-sEYFP₁₋₁₅₄. HeLa cells transfected for 24 h with two plasmids that expressed HA-difopein-sEYFP₁₅₅₋₂₃₈ and Flag-14-3-3ζ-sEYFP₁₋₁₅₄ or Flag-AID-sEYFP₁₋₁₅₄, respectively (0.1, 0.3 or 0.9 μg of each plasmid, x-axis; pcDNA plasmid was added to make up for 2 μg of total DNA). Depicted is the proportion of HeLa cells that were YFP⁺ (one representative of three experiments). **(f)** Immunoblotting analysis of expression of Flag-14-3-3ζ-sEYFP₁₋₁₅₄ or Flag-AID-sEYFP₁₋₁₅₄ in HeLa cells transfected for 24 h. **(g)** BiFC assays of direct interaction of 14-3-3β, 14-3-3ε, 14-3-3γ, 14-3-3η, 14-3-3σ, 14-3-3τ and 14-3-3ζ with PKA-Cα in HeLa cells (one representative of three experiments).



Supplementary Figure 9. 14-3-3 enhance AID-mediated (dC) DNA deamination in a dose-dependent fashion. **(a)** Schematics of the AID deamination assay. Purified recombinant GST-AID deaminates dC residues of Alexa Fluor 647-labeled [5'-AGCT-3']₃-24 nt oligonucleotide (5'-AGCTAAAAAGCTAAAAAGCTAAAA-3') to generate dUs, which were in turn deglycosylated by Ung to generate abasic sites. Following Alkaline/heat treatment-mediated abasic site cleavage, the intact substrate and cleavage products were fractionated in denaturing 15% PAGE containing 8 M urea and visualized using a Typhoon™ 9410 scanner. The intensity of substrate and cleavage product bands was quantified by ImageQuant™ TL software to calculate the percentage of DNA substrate (dC) deaminated (sum of three cleavage products over the total input DNA). y-axis). **(b)** The percentage of DNA substrate (dC) deaminated (y-axis) by purified recombinant GST-AID (0.2 – 20 ng, x-axis). **(c)** Purified recombinant GST-AID (1, 2 and 5 ng) deaminated Alexa Fluor 647-labeled [5'-AGCT-3']₃-24 nt oligonucleotide in the presence of different amounts of purified recombinant GST-14-3-3γ, GST-14-3-3σ, or GST-14-3-3ζ (x-axis). The enhancement of AID-mediated dC deamination by 14-3-3γ, 14-3-3σ or 14-3-3ζ is expressed as percentage of increase (y-axis) of proportion of DNA substrate deaminated in the presence of GST-14-3-3γ (upper panel), GST-14-3-3σ (middle panel) or GST-14-3-3ζ (lower panel), respectively, over that in the presence of GST controls.

Supplementary Table 1. Frequency of the 5'-AGCT-3' occurrence in *IgH* S region DNA

Human ^a			Mouse ^b		
S μ	19.23% ^c	4,534 bp ^d	S μ	20.97% ^c	4,025 bp ^d
S γ 3	5.29%	3,405 bp	S γ 3	9.03%	4,917 bp
S γ 1	4.59%	4,357 bp	S γ 1	5.98%	9,236 bp
S $\psi\epsilon$	7.81%	1,945 bp	S γ 2b	9.60%	5,956 bp
S α 1	18.73%	3,501 bp	S γ 2a	7.68%	5,674 bp
S γ 2	3.15%	3,814 bp	S ϵ	11.93%	2,883 bp
S γ 4	3.28%	4,757 bp	S α	16.28%	4,177 bp
S ϵ	10.82%	2,773 bp			
S α 2	13.49%	3,322 bp			
C μ ^e	1.21%	4,286 bp	C μ ^e	1.23%	3,904 bp

^aRefSeq accession number NC_000014.7.

^bRefSeq accession number NG_005838.1.

^cFrequency of the 5'-AGCT-3' motif, as percentage of S or C μ region DNA.

^dLength of S or C μ region DNA analyzed. The core of each S region contains a higher frequency of 5'-AGCT-3' repeats.

^eGenomic DNA encompassing C μ exons C $_H$ 1, C $_H$ 2, C $_H$ 3, C $_H$ 4-S, M1 and M2 and their introns.

Supplementary Table 2. Binding of 14-3-3 proteins in human B cells to the [5'-AGCT-3']₃-24 bp oligonucleotide.

Protein ¹	Relative amount (relative to the total proteins) ²	Molecular weight (kD)
14-3-3 proteins ³		
14-3-3β	2.1%	28.1
14-3-3ε	18.6%	29.2
14-3-3γ	7.5%	28.3
14-3-3η	4.1%	28.2
14-3-3σ	0.2%	27.8
14-3-3τ	4.8%	27.8
14-3-3ζ	13.4%	27.8
Subtotal (14-3-3 proteins)	50.7% ⁴	
Non-14-3-3 proteins		
SET translocation gene	3.9%	32.1
β-tubulin	2.7%	49.7
Acidic (leucine-rich) nuclear phosphoprotein 32 family, member E	2.4%	30.7
Nucleolin	1.6%	76.3
Acidic (leucine-rich) nuclear phosphoprotein 32 family, member A	1.4%	28.6
Nudix-type motif 5	1.0%	24.3
Protein phosphatase 1	1.0%	41.6
Ribosomal protein P2	0.9%	11.7
Calumenin precursor	0.9%	37.1
Ribosomal protein P1	0.8%	11.5
Proliferating cell nuclear antigen	0.8%	28.8
Myotrophin	0.8%	12.9
Phosphohistidine phosphatase 1	0.8%	13.8
Endonexin II	0.8%	35.9
RAN binding protein 1	0.7%	14.4
Smooth muscle and non-muscle myosin alkali light chain isoform 1	0.6%	16.9
Thioredoxin	0.6%	18.1
F-box and leucine-rich repeat protein 6, isoform 1	0.6%	58.6
Autoantigen La	0.5%	46.8
High-mobility group protein 1-like protein	0.5%	26.8
Subtotal (20 most abundant non-14-3-3 proteins)	23.1%	
Subtotal (the remaining 167 non-14-3-3 proteins)	26.2%	

1. Nuclear proteins from human 4B6 B cells were subjected to purification using an affinity column bearing the [5'-AGCT-3']₃-24 bp oligonucleotide. Eluted proteins were digested to generate peptides for MudPIT analysis (Exp. 3, representative of three independent experiments).

2. Relative amount of a protein (to the total proteins) is defined as the ratio of the peptides that were derived from one protein to the total identified peptides and expressed as percentage (%) of the total proteins. The low relative amount of 14-3-3σ might result from its low expression in 4B6 B cells.

3. The sequence coverage of the seven 14-3-3 isoforms, as defined by the proportion of amino acids of each isoform covered by both isoform-unique peptides and peptides common to other isoform(s), was as follows (numbers inside parentheses indicate the proportion of amino acids of each isoform covered by isoform-unique peptides only): 14-3-3β, 76.8% (59.3%); 14-3-3ε, 64.7% (52.1%); 14-3-3γ, 55.1% (49.8%); 14-3-3η, 58.5% (52.4%); 14-3-3σ, 32.5% (27.1%); 14-3-3τ, 48.6% (38.8%); 14-3-3ζ, 75.5% (69.5%).

4. In the two other independent affinity purification/MudPIT experiments, 14-3-3 proteins accounted for 52.8% and 59.2% of the total amount of eluted proteins.

Supplementary Table 3. Oligonucleotide sequences.

		Forward primer	Reverse primer	Size of PCR products
ChIP assay				
Human				
	S μ	5'- ATGGAAGCCAGCCTGGCTGT -3'	5'- CAGTTAGTGCAGCCAAGCCCTAGCTCAG -3'	210 bps
	S γ 1	5'- ACCCTATGCAGTGTCTGGCCCCTC -3'	5'- AGTCAGCACAGTCCAGTGTCTCTAG -3'	250 bps
	S α			
	(S α 1 and S α 2)	5'- CCTTCTGGAAGCAAAAGGT -3'	5'- TGTTACCTTGTATCCCAGG -3'	200 bps
	C μ	5'- CACGTGGTGTGCAAAGTCCAGCACC -3'	5'- ACGCCAGACCCACCTGCTT -3'	215 bps
	PAX5	5'- AGCACTGCTGCTCTCCCGGCTTCC -3'	5'- TGTGAGATCATGTCCTGTTCTC -3'	195 bps
Mouse				
	S μ	5'- CTGAGGTGATTACTCTGAGGT -3'	5'- CTCCAGAGTATCTCATTTTCAG -3'	265 bps
	S γ 1	5'- CAGGCAAACATAAACAGTGGG -3'	5'-AGGATGTCCACCCCTACCCAGGC -3'	281 bps
	S γ 3	5'-GCTGAGAGTATGCACAGCCA -3'	5'-GGATCATGGAACCTCCTCCG -3'	279 bps
	S α	5'- GGCTGAACTGGGACAAGGTA -3'	5'- CCCATCTCAGCCCAGTTTAT -3'	170 bps
	C μ	5'- GGCTTCTACTTTACCCACAGCATC -3'	5'- CATACACAGAGCAACTGGACACCC -3'	260 bps
RT-PCR analysis				
Human genes				
	<i>AICDA</i>	5'- TGCTCTTCCTCCGCTACATCTC -3'	5'- AACCTCATAACAGGGGCAAAAGG -3'	260 bps
	<i>GAPDH</i>	5'- ACCAACTGCTTAGCACCCCT -3'	5'- CACAGTCTTCTGGGTGGCAG -3'	210 bps
Mouse genes				
	<i>Aicda</i>	5'- TGCTACGTGGTGAAGAGGAG -3'	5'- TCCCAGTCTGAGATGTAGCG -3'	120 bps
	<i>14-3-3β</i>	5'- TGGATAAGAGTGAGCTGGTA -3'	5'- GATCACAGAGCACAACAGAC -3'	735 bps
	<i>14-3-3ϵ</i>	5'- ATTCGGGAGTACCGGCAAAT -3'	5'- GTTCTGTCATCGCAATGTCA C -3'	230 bps
	<i>14-3-3γ</i>	5'- ATCCTCTTCAGCCCTGTGAAG -3'	5'- ATGTGCTCCTTGCTGATCTCGT -3'	570 bps
	<i>14-3-3η</i>	5'- ATATGGCCTCCGCCATGAAGG -3'	5'- GAACTTGTCAAGCAGAGCCA A -3'	245 bps
	<i>14-3-3σ</i>	5'- AGAACCCAGCGTTACTCTCG A -3'	5'- CCACCACGTTCTTGTAAGCT -3'	210 bps
	<i>14-3-3τ</i>	5'- AAGACCGAGCTGATCCAGAA -3'	5'- GGCTCCTTGGGAATTTTCTA T -3'	430 bps
	<i>14-3-3ζ</i>	5'- TTGAGCAGAAGACGGAAGGT -3'	5'- CCTTTCTTGTCATCACCAGC -3'	225 bps
	<i>Gapdh</i>	5'- TTCACCACCATGGAGAAGGC -3'	5'- GGCATGGACTGTGGTCATGA -3'	215 bps
Genotyping				
<i>14-3-3$\gamma^{+/-}$</i>				
	WT allele	5'- CCACGACTGTCCTGTCTTTGATTG -3'	5'- CCTTACTGGAACACAGAACGC -3'	230 bps
	KO allele	5'- TGAGGAGAGAACTGGCTGAGTGAC -3'	5'- CCTTACTGGAACACAGAACGC -3'	340 bps
<i>14-3-3$\sigma^{+/Er}$</i>				
	WT and Er alleles	5'- CTGCTGCAGCGATTCTCTC -3'	5'- TCAGGCACCTAAGTACATGTGC -3'	WT: 104 bps Er: 82 bps

Supplementary Table 4. Antibodies.

Antibody to	Type	Company	Cat. No.	Assays
14-3-3	Rabbit pAb	Abcam	ab6081	IB, IP, ChIP, IF, IHC, EMSA
14-3-3	Rabbit pAb	Abcam	ab9063	EMSA
14-3-3	Rabbit pAb	Santa Cruz Biotechnology	sc-629	EMSA
14-3-3	Rabbit pAb	Santa Cruz Biotechnology	sc-13959	EMSA
14-3-3	Mouse mAb	Abcam	ab14121	IB
14-3-3 β	Rabbit mAb	Abcam	ab32560	EMSA
14-3-3 β	Mouse mAb	Gene Tex, Inc.	GTX-12341	IB
14-3-3 ϵ	Rabbit pAb	Santa Cruz Biotechnology	sc-1020	IB
14-3-3 γ	Rabbit pAb	IBL, Inc.	IBL-18647	IB, ChIP
14-3-3 η	Rabbit pAb	IBL, Inc.	IBL-18645	IB
14-3-3 η	Mouse mAb	Upstate/Millipore	05-632	IB, ChIP
14-3-3 τ	Rabbit pAb	Santa Cruz Biotechnology	sc-732	IB
14-3-3 ζ	Rabbit pAb	Santa Cruz Biotechnology	sc-1019	IB, IP
AID	Mouse mAb	Invitrogen	39-2500	IB, IP, ChIP, IF, IHC
PKA-C α	Rabbit pAb	Santa Cruz Biotechnology	sc-093	ChIP
PCNA	Mouse mAb	BD Pharmingen	555566	IB, IP, IF
Ku86	Mouse mAb	NeoMarkers	MS-285-P1	IB, IP, IF
RPA p34	Mouse mAb	NeoMarkers	MS-691-P1	ChIP, IF
BCL6	Mouse mAb	Dako	M7211	IHC
Mouse IgG, peroxidase-conjugated	Goat pAb	Dako	P0448	IHC
Rabbit IgG, peroxidase-conjugated	Goat pAb	Dako	P0447	IHC
Flag	Mouse mAb	Sigma	F3165	IB
β -actin	Mouse mAb	Sigma	A5441	IB
Mouse IgG (H+L), Rodamine-conjugated	Goat pAb	Pierce	31661	IF
Mouse IgG, TRITC-conjugated	Goat pAb	KPL	03-18-06	IF
Rabbit IgG, FITC-	Goat pAb	KPL	172-1506	IF
Mouse IgG, Alexa Fluor 594-conjugated	Goat pAb	Invitrogen	A-11005	IF
Rabbit IgG, Alexa Fluor 488-conjugated	Goat pAb	Invitrogen	A-11008	IF
Human/mouse CD45R (B220), PE-conjugated	Rat mAb	eBioscience	25-0452-83	FCM, CS
Human CD19, PE-conjugated	Mouse mAb	Sigma	F-3899	FCM, CS
Human CD19, FITC-conjugated	Mouse mAb	eBioscience	11-0199-73	FCM, CS
Human CD19, Biotin-conjugated	Mouse mAb	BD Pharmingen	555411	FCM, CS
Human CD38, FITC-conjugated	Mouse mAb	BD Pharmingen	555459	FCM, CS
Human CD38, PE-conjugated	Mouse mAb	BD Pharmingen	31015X	FCM, CS
Human IgD, Biotin-conjugated	Goat pAb	Southern Biotech	20320	FCM, CS
Human IgM, Biotin-conjugated	Goat pAb	Sigma	B-1265	FCM
Human IgM, FITC-conjugated	Goat pAb	Sigma	F-5384	FCM
Human IgG, APC-conjugated	Mouse mAb	BD Pharmingen	550931	FCM
Human IgG, Biotin-conjugated	Mouse mAb	BD Pharmingen	555785	FCM
Human IgA, FITC-conjugated	Goat pAb	Sigma	F-5259	FCM, CS
Human IgA, Biotin-conjugated	Goat pAb	Southern Biotech	205-208	FCM, CS
Human CD25 (IL-2R), Biotin-conjugated	Mouse mAb	eBioscience	13-0259-82	FCM
Mouse CD45R (B220), APC-conjugated	Rat mAb	BD Pharmingen	553092	FCM, CS
Mouse IgG1, APC-conjugated	Rat mAb	BD Pharmingen	550874	FCM
Mouse IgG3, FITC-conjugated	Rat mAb	BD Biosciences	553403	FCM
Mouse IgG1, FITC-conjugated	Rat mAb	BD Pharmingen	553443	FCM
Mouse IgG2b, FITC-conjugated	Rat mAb	BD Pharmingen	553395	FCM
Mouse IgA, FITC-conjugated	Rat mAb	BD Pharmingen	559354	FCM
Mouse IgG2a, FITC-conjugated	Rat mAb	BD Pharmingen	553390	FCM
Mouse IgM, FITC-conjugated	Rat mAb	BD Pharmingen	553437	FCM
non-specific	Rabbit pAb	Santa Cruz Biotechnology	sc-2027	IB, IP, ChIP, IF
non-specific	Mouse pAb	Santa Cruz Biotechnology	sc-2025	IB, IP, ChIP, IF

Abbreviations: mAb, monoclonal antibody; pAb, polyclonal antibody;
ChIP, chromatin immunoprecipitation; CS, cell sorting; EMSA, electrophoretic mobility shift assay; FCM, flow cytometry; IB,
immunoblotting; IF, immunofluorescence; IHC, immunohistochemistry; IP, immunoprecipitation.

Supplementary Methods.

Co-IP assays. Co-IP assays were performed as we described (Connaghan-Jones et al., *J. Biol. Chem.*, 279: 42258–42269, 2004). In assays involving DNase I treatment prior to immunoprecipitation, cell lysates were prepared in EDTA-free lysis buffer and incubated with 20 unit ml⁻¹ DNase I (Qiagen) in the presence of 10 mM MgCl₂ at 32°C for 3 h before immunoprecipitation. For pull-down of 14-3-3 and His₁₀-Flag₂-AID, 2 × 10⁶ human 4B6 B cells grown to the mid-logarithmic phase (6 × 10⁵ cell ml⁻¹) were resuspended in 100 µl Human B Cell Nucleofector Solution (Amaxa Inc.), mixed with 5 µg plasmid that encodes His₁₀-Flag₂-AID, or the empty vector pcDNA3, and electroporated in the Nucleofector II device (Amaxa Inc.) using the program U-15 per manufacturer's instructions. Transfected cells were then cultured for 24 h and whole cell lysates were precipitated by Ni-NTA magnetic agarose beads (Qiagen) following manufacturer's instructions.

DNase I footprint assays. DNase I footprint assays were performed as described (Connaghan-Jones et al., *Nat. Protoc.*, 3: 900–914, 2008) with minor modifications. The 126-bp double-strand DNA fragment (Alexa Fluor 647–5'-GAGAGATGGATAATACGACTCACTATAGGGAGAAAAGGGGAAAGCTAAAAAGCTAAAAAGCTAAAAGAGGAAAGGTGAGGAGGTCTGGTGGCCATGGTCTGTCTAGACAGACTGTTCGAAGTACTGA-3', only one strand was labeled with Alexa Fluor 647 at the 5' end) was incubated with purified recombinant GST-tagged 14-3-3 isoforms (14-3-3γ, 14-3-3σ or 14-3-3ζ) or control BSA or BSA plus GST in the reaction buffer (45 µl, 10 mM Tris–HCl, pH 8.0, 5 mM MgCl₂, 1 mM CaCl₂, 2 mM DTT) for 60 m at 25°C before digestion by 0.000016 Kunitz unit µl⁻¹ of DNase I in 50 µl of reaction mixture at 25°C. After 2 m, the reaction was stopped by addition of 350 µl of stop solution (80% ethanol, 0.5 M NH₄Ac, 5 µg of tRNA). After precipitation in a dry ice-ethanol bath for 15 m, the DNA pellet was washed with 70% ethanol and resuspended in 20 µl of loading buffer (95% formamide, 20 mM EDTA). After heating at 95°C for 5 m and chilling on ice, samples were applied to a denaturing 6% polyacrylamide gel containing 7 M urea, run for 2 h at 60 W and then visualized using a Typhoon™ 9410 scanner (GE Healthcare).

EMSA. Preparation of nuclear extracts from human 4B6 or 2E2 B cells were described (Park et al., *Nat. Immunol.* 10, 540–550, 2009). In EMSA assays, nuclear extracts were incubated with 12 nM of ³²P- or Alexa Fluor 647-labeled oligonucleotide probe in a buffer consisted of 20 mM HEPES, pH 7.9, 4 mM MgCl₂, 1 mM EDTA and 0.05% NP-40 in the presence of 150 mM KCl and 100 µg ml⁻¹ poly(dI/dC), which inhibited non-specific binding of proteins to DNA, at 25°C for 30 m. Protein/DNA complexes were run on 7% native PAGE for typically 6.5 h and visualized by autoradiogram (for ³²P-labeled probes) or using a Typhoon™ 9410 scanner (for Alexa Fluor 647-labeled probes). In EMSA blocking/supershift assays, nuclear extracts were incubated with rabbit IgG Ab recognizing all 14-3-3 isoforms (Ab1, ab6081, Abcam; Ab2, sc-629, Santa Cruz Biotechnology; Ab3, sc-13959, Santa Cruz Biotechnology; and Ab4, ab9063, Abcam), 14-3-3β (ab32560, Abcam), 14-3-3ζ (sc-1019, Santa Cruz Biotechnology) or pre-immune rabbit IgG as irrelevant Ab at 25°C for 10 m before binding to the [5'-AGCT-3']₃-24 bp probe.

Immunohistochemistry. Paraffin-embedded human tonsil surgical specimens were sectioned with a cryostat at 6 µm onto glass slides. After de-paraffinization and re-hydration, slides were processed following a typical staining procedure involving specific primary antibodies and peroxidase labeled polymer conjugated with goat anti-mouse or goat anti-rabbit IgG as secondary Abs (Dako). After color development using the DAB+ chromogen (Dako), slides were dehydrated and counterstained with hematoxylin before examination by microscopy. Immunofluorescence staining of mouse spleen germinal centers was as we described (Park et al., *Nat. Immunol.* 10, 540–550, 2009) and all fluorescence pictures were pseudo-colored.

MudPIT. The three main elution fractions (#3, #4 and #5) were pooled and concentrated using a Centricon YM-3 centrifugal filter (Millipore) before precipitation by trichloroacetic acid and washing with acetone. Protein pellets were solubilized in 100 mM Tris–HCl (pH 8.5) and 8 M urea and then reduced by 5 mM Tris (2-carboxyethyl) phosphine hydrochloride and carboxyamidomethylate in 10 mM iodoacetamide. After digestion with Lys-C endopeptidase for 4 h at 37°C, samples were diluted to 2 M urea with 100 mM Tris–HCl (pH 8.5) and 1 mM CaCl₂ for trypsin digestion overnight at 37°C. After neutralization of trypsin with 5% formic acid, acidified peptide samples were sequentially separated by a strong cation exchange column and then a reverse phase HPLC (Hewlett-Packard) before mass spectrometry (MS) analysis using a LCQ ion trap mass spectrometer equipped with nano-LC electrospray ionization source (Finnigan). For peptide identification, MS spectra were analyzed for homology to the human translated genomic database from the National Center for Biotechnology Information (NCBI) using SEQUEST algorithm. For protein identification, the SEQUEST outputs were analyzed by DTASelect software. Four or more peptides passing DTASelect filters and covering non-overlapping regions of a protein would identify this protein as an automatic hit. Proteins identified by one to three non-overlapping peptides passing DTASelect filters were manually validated and only those with at least 10% sequence coverage (defined as the proportion of total amino acids of a protein covered by peptides identified) were considered real hits. Relative amount of a protein (relative to the total proteins) is defined as the ratio of the peptides that were derived from one protein to the total identified peptides and expressed as percentage (%) of the total proteins.

Oligonucleotides and antibodies. The sequences of oligonucleotides used for ChIP, RT-PCR and genotyping are listed in **Supplementary Table 3**. Those of oligonucleotides used for real-time qRT-PCR of *IgH* transcripts were reported (Park et al., *Nat. Immunol.* 10, 540–550, 2009). Abs are listed in **Supplementary Table 4**.

RT-PCR and quantitative real-time RT-PCR (qRT-PCR). RNA extraction and first strand cDNA synthesis, RT-PCR and SYBR green-based real-time qRT-PCR analysis were as described (Park et al., *Nat. Immunol.* 10, 540–550, 2009).